CrossMark

ORIGINAL PAPER

Nonlinear dynamic analysis and fatigue damage assessment for a deepwater test string subjected to random loads

Kang Liu[1] · Guo-Ming Chen[1] · Yuan-Jiang Chang[1] · Ben-Rui Zhu[1] ·
Xiu-Quan Liu[1] · Bin-Bin Han[1]

Abstract The deepwater test string is an important but vulnerable component in offshore petroleum exploration, and its durability significantly affects the success of deepwater test operations. Considering the influence of random waves and the interaction between the test string and the riser, a time-domain nonlinear dynamic model of a deepwater test string is developed. The stress-time history of the test string is obtained to study vibration mechanisms and fatigue development in the test string. Several recommendations for reducing damage are proposed. The results indicate that the amplitude of dynamic response when the string is subjected to random loads gradually decreases along the test string, and that the von Mises stress is higher in the string sections near the top of the test string and the flex joints. In addition, the fatigue damage fluctuates with the water depth, and the maximum damage occurs in string sections adjacent to the lower flex joint and in the splash zone. Several measures are proposed to improve the operational safety of deepwater test strings: applying greater top tension, operating in a favorable marine environment, managing the order of the test string joints, and performing nondestructive testing of components at vulnerable positions.

✉ Guo-Ming Chen
offshore@126.com

Kang Liu
lkzsww@163.com

[1] Centre for Offshore Engineering and Safety Technology, China University of Petroleum, Qingdao 266580, Shandong, China

1 Introduction

In recent years, the deepwater drilling unit HYSY981, which is operated by the China National Offshore Oil Corporation (CNOOC), has drilled several exploration wells in the South China Sea (Xu et al. 2013). Petroleum exploration in China has gradually progressed from near-shore to deepwater locations (Chen et al. 2013; Hu et al. 2013). The deepwater test string is a crucial component used for assessing the formation fluid characteristics and potential production of wells during the early stage of offshore petroleum exploration. However, for the complexity of testing process, marine environment and structure of the string, vibration and fatigue that occur in a deepwater test string are not fully understood. Therefore, the study of nonlinear vibration dynamics and fatigue damage in deepwater test strings is of great scientific and engineering significance.

A deepwater test string is inevitably subjected to rapid currents and waves resulting in wear and fatigue due to friction and collision with the riser. However, previous studies have primarily focused on wave-induced fatigue (Nazir et al. 2008; Khan and Ahmad 2010; Li and Low 2012) and vortex-induced fatigue (Yang et al. 2007; Tognarelli et al. 2010; Song et al. 2011) for a single-layer deepwater string, such as a drilling riser and production riser. There has been little research on the coupling dynamics of deepwater test strings and risers at present. Only a few studies have focused on extrusion and contact analysis of offshore double-layer strings in construction and installation (Wang et al. 2009; Chen and Chia 2010).

Currently, studies of nonlinear contact analysis of downhole oil/drill pipe (Pang et al. 2009; Dong et al. 2012) and multistring analysis (Liu et al. 2014b) are available for reference. In the study of test strings, some researchers have focused on deepwater job safety analysis and risk control techniques (Stomp et al. 2005; Chen et al. 2008; Mogbo 2010; Wendler and Scott 2012), while others have focused on mechanical analysis, design optimization, axial deformation, and other aspects of the downhole string (Zeng et al. 2010; Li 2012; Cheng et al. 2014). Liu et al. (2014a) studied the limits of platform offset for a deepwater test string, but its static and dynamic mechanical behavior have not been evaluated. Xie et al. (2011) studied the dynamics of a deepwater test string based on the top boundary simulation, but the interaction between the test strings and the riser and fatigue damage were not investigated.

An equivalent composite model is often used to analyze deepwater double-layer hydrocarbon strings. In this model, it is assumed that the pipes move together uniformly under external and internal loading, and the equivalent pipe bending and tension are shared equally based on the stiffness and the bearing area of the pipes. This model can be used to analyze motion, but is likely to be inaccurate in fatigue damage evaluation (Harrison and Helle 2007). To study the interaction between the test string and the riser, and the structural response of a deepwater test string in various operating modes, a model of the nonlinear dynamics for a deepwater test string is developed. Vibration and damage in deepwater test strings are studied to provide guidelines for structural design and operation management.

2 Nonlinear dynamic model

Deepwater well testing is generally conducted on a floating platform, as illustrated in Fig. 1. The top tension of the riser and the test string are provided by a tensioner and a hook, respectively. The riser and the conductor comprise the outer string system with connection of the wellhead, forming a circulation channel for testing fluid. The inner string system is composed of oil tube/drill pipe, centralizer, subsea test tree, and fluted hanger (Bavidge 2013), forming a passage for hydrocarbons from the sea floor to the platform, which can be used to measure and control the test parameters. The entire deepwater test string system is not only subjected to various external loads (e.g., waves, currents, and platform movement) but also random contact and collision between the test string and the riser.
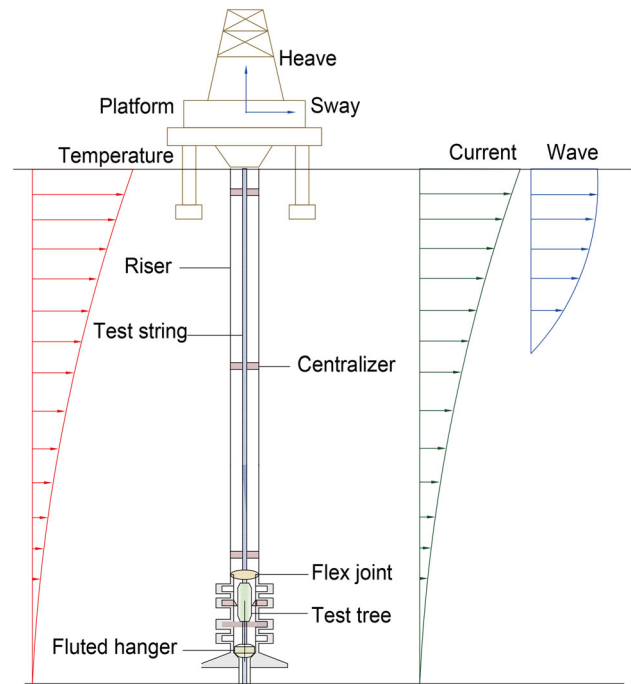

Fig. 1 Schematic diagram for the deepwater test string system

The dynamics of the deepwater test string and the riser are expressed using the partial differential equation of a beam in a vertical plane (Park and Jung 2002)

$$\frac{\partial^2}{\partial z^2}\left(EI\frac{\partial^2 y}{\partial z^2}\right) - \frac{\partial}{\partial z}\left(T\frac{\partial y}{\partial z}\right) + c\frac{\partial y}{\partial t} + m\frac{\partial^2 y}{\partial t^2} = F(z,\ t), \quad (1)$$

where z is the vertical height, m; y is the horizontal displacement, m; E is the elastic modulus, Pa; I is the moment of inertia, m^4; T is the effective tension, N; c is the damping factor of the structure, N s/m; m is the mass of the string per unit length, kg; t is time, s; and F is the transverse load per unit length, including environmental loads and contact forces between the test string and the riser, N.

The test string makes contact with riser due to the action of waves and currents in deepwater operations. Thus, a pipe-in-pipe model is used to simulate the interaction between the test string and the riser. In Fig. 2, the blue area represents the riser, the red area represents the test string, and the green area represents the gap element that constrains the riser and the test string.

The displacement vector at any point on the test string is denoted by

$$U_i = [w_i, v_i, \theta_i], \quad (2)$$

where w_i and v_i represent linear displacements in the local coordinate system, m; and θ_i represents the angular displacement, rad.
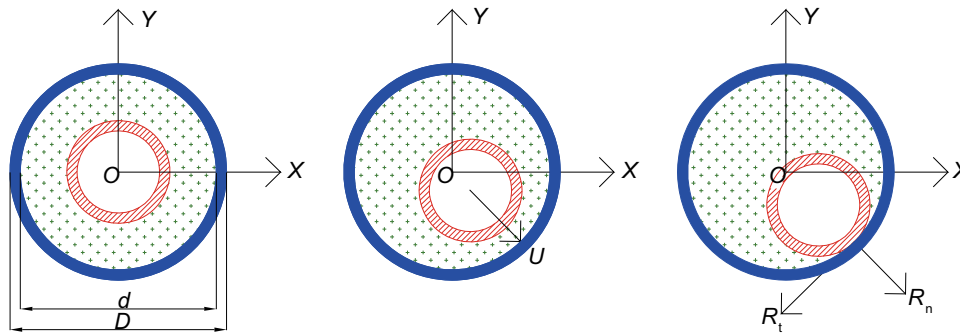
Fig. 2 The contact model for test string and riser

Applying the law of conservation of momentum and the theory of tube-string mechanics, the contact–impact model for the test string and the riser is given by

$$R_{ni} = \begin{cases} m(1-e)\sqrt{\dot{w}_i^2 + \dot{v}_i^2} \big/ \Delta t & \left(\sqrt{\dot{w}_i^2 + \dot{v}_i^2} > \varepsilon, \text{ collision}\right) \\ -T_{ni} & \left(\sqrt{\dot{w}_i^2 + \dot{v}_i^2} < \varepsilon, \text{ contact}\right) \end{cases},$$
$$R_{ti} = \mu R_{ni}$$
$$M_i = d_i R_{ti}/2$$
(3)

where R_{ni} and R_{ti} represent the normal force and the friction force between the test string and the riser at the ith gap element, N; M_i is the moment of the friction, N m; m is the mass of the string per unit length, kg; e is the restitution coefficient of collision, which is obtained from experiment, and we set $e = 0.58$ in this paper; Δt is the duration of the collision, s; T_{ni} is the reaction force, N; ε is the speed threshold value of the collision and contact, m/s; μ is the friction coefficient, and we set $\mu = 0.25$ in this paper; and d_i is the inner diameter of the riser, m.

Based on these equations, a finite element model of the nonlinear dynamics for the deepwater test string system is obtained

$$\begin{cases} \mathbf{M}_t \ddot{\mathbf{U}}_t + \mathbf{C}_t \dot{\mathbf{U}}_t + \mathbf{K}_t \mathbf{U}_t = \mathbf{F}_t + \mathbf{f}(\mathbf{U}_t, \mathbf{U}_r) \\ \mathbf{M}_r \ddot{\mathbf{U}}_r + \mathbf{C}_r \dot{\mathbf{U}}_r + \mathbf{K}_r \mathbf{U}_r = \mathbf{F}_r - \mathbf{f}(\mathbf{U}_t, \mathbf{U}_r) \end{cases},$$
(4)

where $\mathbf{M}_t$ and $\mathbf{M}_r$ represent the mass matrixes of the test string and the riser, respectively, kg; $\mathbf{C}_t$ and $\mathbf{C}_r$ represent the damping matrixes of the test string and the riser, respectively, N s/m; $\mathbf{K}_t$ and $\mathbf{K}_r$ represent the stiffness matrixes of the test string and the riser, respectively, N/m; $\mathbf{U}_t$ and $\mathbf{U}_r$ represent the global displacement vectors of the test string and the riser, respectively, m; $\mathbf{F}_t$ is the force vector of the test string including the effective weight of the test string and the internal fluid, N; $\mathbf{F}_r$ is the force vector of the riser including both the effective weight of riser, annular fluid, and auxiliary lines and the transverse

loads of random waves and currents, N; $\mathbf{f}(\mathbf{U}_t, \mathbf{U}_r)$ represents the contact or impact load of the test string and the riser, N.

3 Nonlinear vibration induced by waves

3.1 Wave-induced vibration mechanism

Waves and the motion of floating platform are the main loads that drive the dynamic response of a deepwater test string. The boundary condition is given by the wave frequency and the low-frequency motion of the platform due to waves. Currents act on the riser directly, and loads are transmitted to the test string via the gap element, which primarily affects the time-invariant portion in the dynamic response of the test string. Waves affect the dynamic response of a test string in two ways: (1) they produce hydrodynamic loads on the riser, which are transmitted to the test string via the gap element; (2) they cause the floating platform to move, which is modeled through the response amplitude operator (RAO), and form the moving boundary condition at the top of the test string. Figure 3 shows the effects of waves on the deepwater test string system.

The wave spectrum is typically used to simulate ocean waves. In this paper, the P–M spectrum is used. The loads on the deepwater test string system caused by waves are calculated using the Morison equation (Morooka et al. 2005). Simulation of the motion of the floating platform is an essential part of the vibration analysis of the deepwater test string system. Including the effect of long-term drift, the motion of the floating platform is represented as follows (Chang et al. 2008):

$$S(t) = S_0 + S_1 \sin\left(\frac{2\pi t}{T_1} - \alpha_1\right)$$
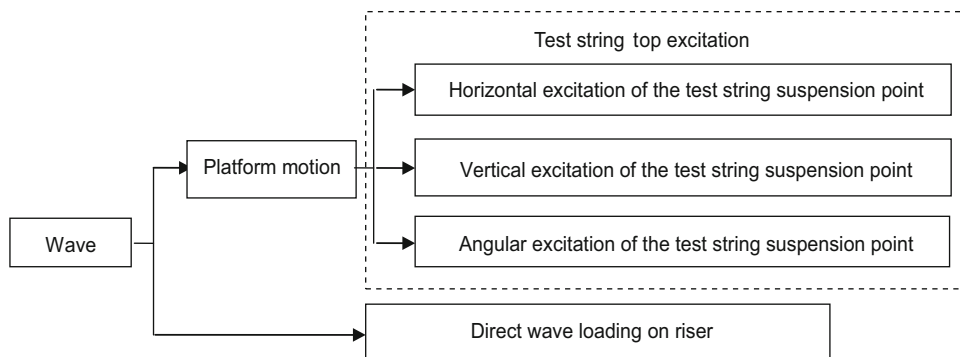$$+ \sum_{n=1}^{N} S_n \cos(k_n x - \omega_n t + \varphi_n + \alpha_n),$$
(5)

Fig. 3 Effects of waves on the deepwater test string system

where $S(t)$ is the time-dependent platform motion response, m; S_0 is the mean platform offset, m; S_1 is the single amplitude of the platform drift, m; T_1 is the period of platform drift motion, s; α_1 is a phase angle difference between the drift motion and the wave, rad; S_n is the amplitude of the nth wave component, m; k_n, ω_n, and φ_n are the wave number, frequency, and phase angle of the nth wave component, respectively, m^{-1}, Hz, rad; and α_n is the phase angle of the RAO, rad.

Assuming a platform drift amplitude of 10 m, a long-term platform drift period of 250 s, and a significant wave height of 4 m, the time history of floating platform motion is obtained using the method described previously; the results are shown in Fig. 4.

3.2 Dynamic response analysis

A deepwater well at a depth of 1500 m in the South China Sea was studied as an example. The configurations of the outer and inner string systems are presented in Tables 1 and 2, respectively. The inner string system includes top,
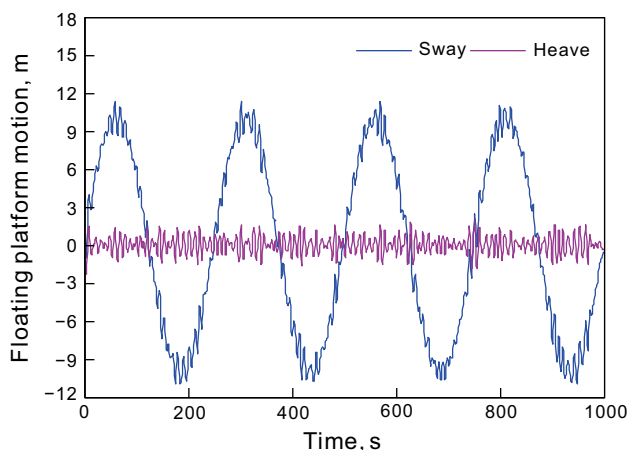

Fig. 4 Time history of floating platform motion

middle, and bottom centralizers used to protect the test sting, a lubricator valve, a subsea test tree, and other critical equipment. The rotational stiffnesses of the upper and lower flex joints in the outer string system are 8.8 and 127.4 kN m/(°), respectively.

Using the motion of the floating platform as a boundary condition, the analysis software ABAQUS Standard and Python were used to simulate the dynamic response of the test string system in the deepwater. The time histories of the flex joint rotation angle, and the von Mises stress envelope of the test string and the riser are shown in Figs. 5 and 6, respectively. Figure 5 shows that the magnitude of the rotation angle for the lower flex joint is much smaller than that for the upper flex joint, which is expected because the rotational stiffness of the former is larger. Moreover, both flex joints rotate in a random pattern, whereas the frequency of the joint rotation remains consistent with the long-term drift motion of the platform. It can be concluded that the platform offset is the dominant factor affecting the flex joint rotation angle.

In Fig. 6, a relative position of 1.0 represents the top of the test string and riser (near the surface of the water), and a relative position of 0 represents the level of the mud line.

Figure 6 shows that (1) the mean value and the amplitude of the von Mises stress tend to decrease gradually along the test string and riser from top to bottom, indicating that the transmission of the vibration at the top of the test string and riser decrease with depth; (2) the von Mises stress of the test string exhibits a sudden decline at points where the cross-sectional areas change, such as at the centralizers, and the stress levels in the corresponding positions of the flex joints increase sharply due to the change of bending moment; (3) the rate of decrease of the von Mises stress in the riser at depths of 120–1216 m generally remains constant with the buoyancy joints; the von Mises stress increases suddenly at 520 m due to the change in wall thickness; the von Mises stress in the riser at 1216–1400 m decreases rapidly because eight slick joints are used; (4) the string sections near the top of the test

Table 1 Configuration of the outer string system

Components	Number of joints	Outside diameter, m	Internal diameter, m	Length of joints, m
Outer barrel of telescopic joint	1	0.6604	0.6096	–
Slick joint 1	2	0.5334	0.4826	22.86
Buoyancy joint 1	20	0.5334	0.489	22.86
Buoyancy joint 2	32	0.5334	0.4826	22.86
Slick joint 2	8	0.5334	0.489	22.86
Buoyancy joint 3	2	0.5334	0.489	22.86
LMRP/BOP	1	–	–	16.288
Wellhead	1	–	–	2
Conductor	1	0.9144	0.87	–

Table 2 Configuration of the inner string system

Components	Outside diameter, m	Internal diameter, m	Length, m
Oil tube	0.1143	0.0857	21.798
Centralizer	0.4064	0.0762	1.29
Lubricator valve	0.3175	0.0762	3.42
Oil tube	0.1143	0.0857	732.48
Centralizer	0.4064	0.0762	1.29
Oil tube	0.1143	0.0857	732.48
Centralizer	0.4064	0.0762	0.97
Retainer valve	0.3175	0.0762	3.73
Tubing	0.1143	0.0857	2.72
Subsea test tree	0.3493	0.0762	1.29
Tubing	0.1143	0.0857	1.55
Fluted hanger	0.3302	0.0762	1.77
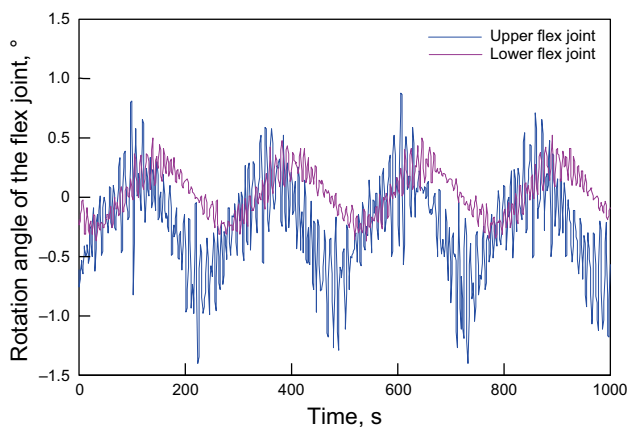
Fig. 5 Time history of the upper and lower flex joints

Fig. 6 The von Mises stress envelope of the deepwater test string and riser

string and flex joints are most prone to damage, so these areas should be given special attention during inspection and maintenance.

The mean contact force between the test string and the riser in a service cycle is displayed in Fig. 7. The following observations regarding the contact force were made: (1) the
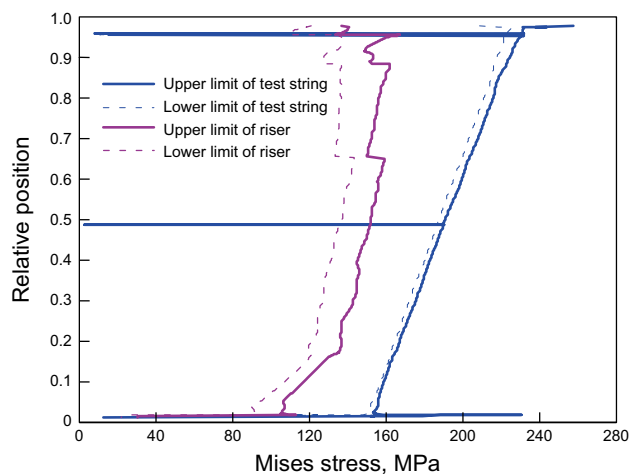
deepwater test string and riser make contact in a random pattern, and the contact forces are relatively larger in the locations corresponding to the flex joints and the
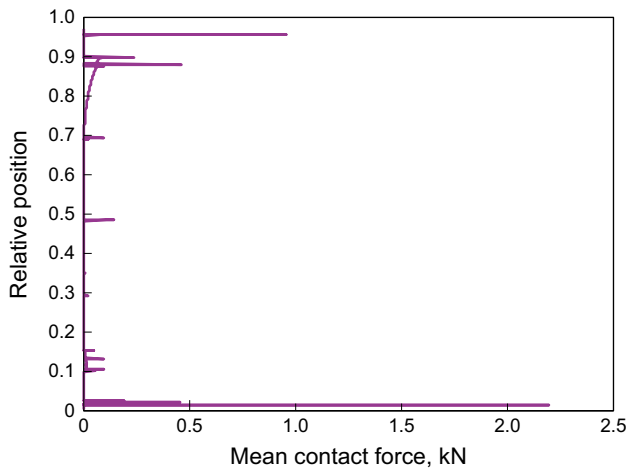
Fig. 7 The mean contact force between the deepwater test string and the riser

centralizers, among which the maximum contact force occurs at the position of the lower flex joint; (2) the mean contact forces are nearly zero in the figure because the gap elements generally do not have a continuous effect on the test string; (3) the contact forces are negligible at the lubricator valve, the retainer valve, and the subsea test tree, because of the effective protection of the centralizers; (4) the part of the test string located in the splash zone bears higher wave loads, whereas the lower part bears greater bending loads, resulting in contact primarily occurring in two areas (depths of 150–450 and 1200–1400 m) apart from the flex joints and the centralizers. Hence, centralizers should be added in those areas to reduce contact. These results have been successfully applied in a deepwater testing operation and have guided preliminary hazard analyses and maintenance for the deepwater test string in the South China Sea.

4 Fatigue analysis induced by waves

4.1 Fatigue damage assessment

The deepwater testing operation runs periodically and typically consists of four stages: deployment/retrieval mode, pressure perforation mode, flowing test mode, and shut-in well mode. These four stages are treated as a service cycle in the fatigue analysis of the deepwater test string system.

Based on the vibration response of the test string under combined loads, a rain-flow counting method (Khosrovaneh and Dowling 1990) was implemented in the MATLAB programming environment to analyze the fatigue damage of the test string in various stages. According

to the linear accumulated damage criterion, the fatigue damage of the test string in a service cycle is calculated as follows:

$$D = \sum_{i,j}^{i=4} \frac{n_{ij}}{N_{ij}} = \sum_{i,j}^{i=4} \frac{n_{ij}S_{ij}^m}{K}, \tag{6}$$

where D is the fatigue damage, a^{-1}; $i = 1$ represents the deployment/retrieval mode, $i = 2$ represents the pressure perforation mode, $i = 3$ represents the flowing test mode, and $i = 4$ represents the shut-in well mode; S_{ij} and n_{ij} represent the fatigue stress amplitude and the cycle index for the corresponding operation modes, respectively; K, m are the S–N curve coefficients, in this paper, we set $m = 3$, and $K = 4.16 \times 10^{11}$.

In deepwater testing, it is common to use high rates of output flowback to prevent the formation of hydrate before downhole sampling and finding production by changing the flow (Triolo et al. 2013). To evaluate wave-induced fatigue damage in the deepwater test string, it was assumed that a service cycle contains: deployment/retrieval for 12 h, perforating for 1 h, flowback testing at 2.92×10^4 m^3/h for 8 h, flowing sampling at 1.25×10^4 m^3/h for 10 h, flowing test at 5.00×10^4 m^3/h for 10 h and at 6.25×10^4 m^3/h for 8 h, and shut-in well for 30 h. The change in flow in flowing testing mode was realized by adjusting the choke, and the shut-in time in transition was negligible.

The fatigue damage to the deepwater test string in the various stages of operation was calculated, as shown in Figs. 8 and 9. The results show that under the influence of waves and floating platform motion, the fatigue damage fluctuates with the water depth. The damage varies considerably with the position, and the maximum damage occurs adjacent to the lower flex joint. For this example,
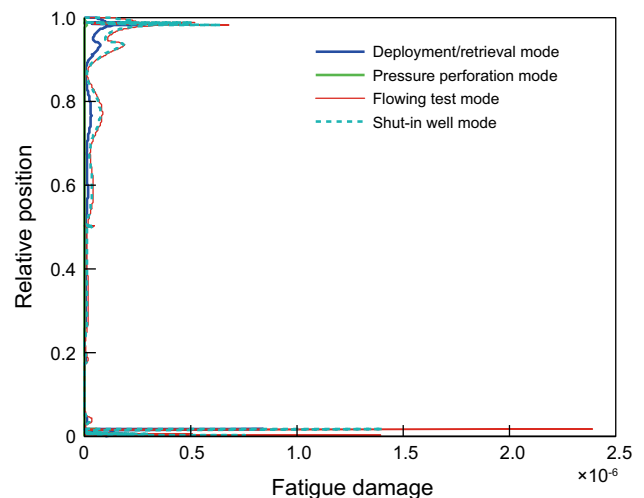

Fig. 8 Fatigue damage in the deepwater test string in different modes
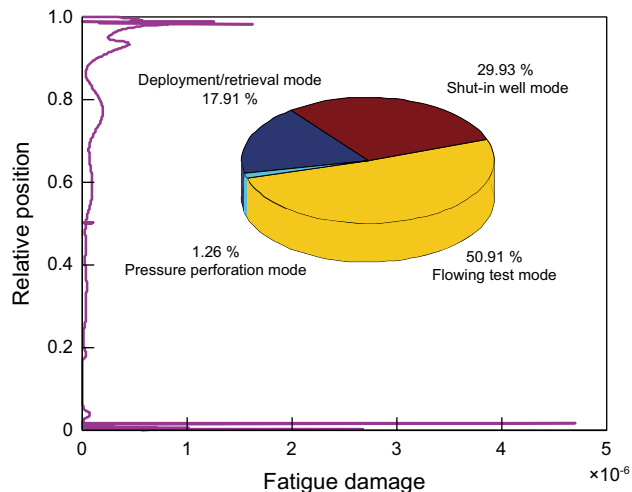
Fig. 9 Fatigue damage in the deep water test string in a typical service cycle

the fatigue damage in the deepwater test string in a service cycle is 4.706e−6, including 8.427e−7 (17.91 %) in the deployment/retrieval mode, 5.910e−8 (1.26 %) in the pressure perforation mode, 2.396e−6 (50.91 %) in the flowing test mode, and 1.409e−6 (29.93 %) in the shut-in well mode.

There are two locations at which the deepwater test system is most susceptible to fatigue: in the vicinity of the splash zone and the lower flex joint. These locations should be given special attention in managing the fatigue life of the deepwater test string. The fatigue damage in the sections located at the top of the test string in the splash zone primarily results from wave loads and the platform heaving motion, whereas the sections adjacent to the lower flex joint are mainly influenced by the offset motion of the floating platform. When the rotational stiffness of the flex joints is lower than that of the riser joints, the bending deformation and the vibration amplitude of the riser and the test string at this position are more significant.

The number of joints in a test string in each service cycle depends on the water depth; thus, the number of joints and their positions will vary. Therefore, the arrangement of the test string should be managed to avoid having the same joints located adjacent to the flex joints in more than one cycle. Moreover, nondestructive testing of the weakness positions should be conducted after each operation, and the damaged joints should be serviced or replaced to ensure that subsequent test operations can be conducted without failure.

4.2 Analysis of contributing factors

Fatigue damage in the deepwater test string is affected most by the top tension and dynamic wave loads. The fatigue resulting from these two factors is shown in Fig. 10.
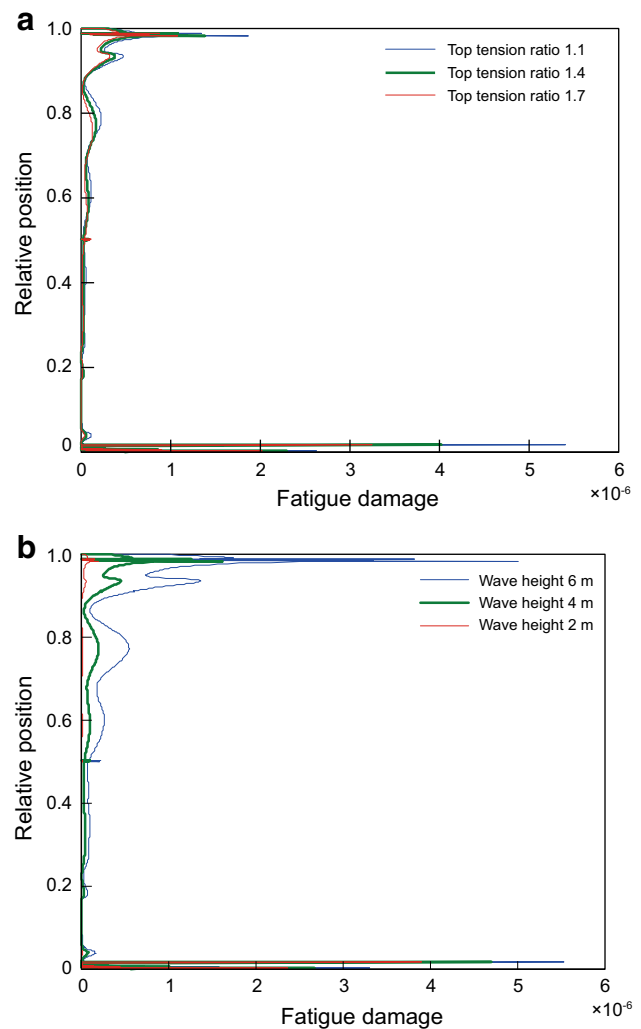

Fig. 10 Fatigue damage in the deepwater test string for two main contributing factor. **a** Fatigue damage for various ratios of top tension. **b** Fatigue damage for various wave heights

As Fig. 10a shows, the fatigue damage tends to decrease with increasing top tension in the riser and the test string, and the fatigue damage in sections adjacent to the flex joints is significant. Higher levels of top tension could decrease the lateral displacement of the test string and the rotation angle of the flex joints, which would reduce the vibration amplitude. Thus, greater top tension could reduce fatigue damage in the test string due to wave action. As Fig. 10b shows, the fatigue damage tends to increase with wave height. The tendency in the upper sections of the test string is quite notable, a consequence of the flow velocity being an exponential function of the water depth. Furthermore, the platform motion caused by waves has a significant influence on the fatigue in the upper sections of the test string. Based on the results of this study, it can be concluded that applying greater top tension and operating in a favorable marine environment would markedly reduce fatigue damage in the test string.

5 Conclusions

(1) A nonlinear dynamic model of pipe-in-pipe configuration for a deepwater test string is established to study the vibration mechanism of a deepwater test string in waves. The results show that the mean value and the amplitude of von Mises stress gradually decrease along the test string. The von Mises stress is lower in locations with larger cross-sectional areas such as the centralizers, whereas the stress is higher in the sections near the top of the test string and the flex joints. The deepwater test string and the riser contact in a random pattern, and the contact loads are relatively larger in the points corresponding to the flex joints and the centralizers. The maximum contact load occurs in the sections adjacent to the lower flex joint.

(2) A fatigue analysis method and procedure are established for analyzing fatigue damage in deepwater test strings subjected to wave action. The results show that the fatigue damage in the deepwater test string fluctuates with the water depth, and damage varies considerably with position. The damage in the sections adjacent to the splash zone and the lower flex joint are much greater. The fatigue damage in the deepwater test string tends to increase as the top tension decreases and with wave height. Moreover, the damage in the flex joint areas is sensitive to the top tension, whereas the damage in the upper sections of the test string is sensitive to the wave height.

(3) Several measures are proposed to improve the operation safety of the deepwater test string. These measures include applying greater top tension and operating in a favorable marine environment to reduce fatigue damage, managing the arrangement of the test string to prevent the test string joints from being placed adjacent to the flex joints in more than one cycle, and performing nondestructive testing of components at vulnerable positions after test operations.

References

Bavidge M. Husky Liwan deepwater subsea control system. In: Offshore technology conference, 6–9 May, Houston; 2013. doi:10.4043/23960-MS.

Chang YJ, Chen GM, Sun YY, et al. Nonlinear dynamic analysis of deepwater drilling risers subjected to random loads. China Ocean Eng. 2008;22(4):683–91.

Chen GM, Liu XQ, Chang YJ, et al. Advances in technology of deepwater drilling riser and wellhead. J China Univ Pet (Ed Nat Sci). 2013;37(5):129–39 (in Chinese).

Chen Q, Chia HK. Pipe-in-pipe walking: understanding the mechanism, evaluating and mitigating the phenomenon. In: ASME 2010 29th international conference on ocean, offshore and arctic engineering, 6–10 June, Shanghai; 2010. doi:10.1115/OMAE2010-20058.

Chen SM, Gong WX, Antle G. DST design for deepwater wells with potential gas hydrate problems. In: Offshore technology conference, 5–8 May, Houston; 2008. doi:10.4043/19162-MS.

Cheng WH, Wang LJ, Li GH. An optimal design of a DST string for high temperature, high pressure and sour gas fields on the Right Bank of the Amu Darya River, Turkmenistan. Nat Gas Ind. 2014;34(4):76–82 (in Chinese).

Dong SM, Zhang WS, Wang Q, et al. Mechanism of eccentric wear between rod string and tubing string of a surface driving screw pump lifting system in vertical wells. Acta Pet Sin. 2012;32(3):304–9 (in Chinese).

Harrison RI, Helle Y. Understanding the response of pipe-in-pipe deepwater riser systems. In: The seventeenth international offshore and polar engineering conference, 1–6 July, Lisbon; 2007.

Hu WR, Bao JW, Hu B. Trend and progress in global oil and gas exploration. Pet Explor Dev. 2013;40(4):439–43. doi:10.1016/S1876-3804(13)60055-5.

Khan RA, Ahmad S. Probabilistic fatigue safety analysis of oil and gas risers under random loads. In: ASME 2010 29th international conference on ocean, offshore and arctic engineering, 6–11, June, Shanghai; 2010. doi:10.1115/OMAE2010-20464.

Khosrovaneh AK, Dowling NE. Fatigue loading history reconstruction based on the rainflow technique. Int J Fatigue. 1990;12(2):99–106. doi:10.1016/0142-1123(90)90679-9.

Li FZ, Low YM. Fatigue reliability analysis of a steel catenary riser at the touchdown point incorporating soil model uncertainties. Appl Ocean Res. 2012;38(1):100–10. doi:10.1016/j.apor.2012.07.005.

Li ZF. Mechanical analysis of tubing string in well testing operation. J Pet Sci Eng. 2012;90(91):61–9. doi:10.1016/j.petrol.2012.04.019.

Liu K, Chen GM, Chang YJ, et al. Warning control boundary of platform offset in deepwater test string. Acta Pet Sin. 2014a;35(6):1204–10 (in Chinese).

Liu XQ, Chen GM, Chang YJ, et al. Multistring analysis of wellhead movement and uncemented casing strength in offshore oil and gas wells. Pet Sci. 2014b;11(1):131–8. doi:10.1007/s12182-014-0324-7.

Mogbo O. Deepwater DST design, planning and operations-Offshore Niger Delta experience. In: Production and operations conference and exhibition, 8–10 June, Tunis; 2010. doi:10.2118/133772-MS.

Morooka CK, Coelho FM, Ribeiro EJB, et al. Dynamic behavior of a vertical riser and service life reduction. In: ASME 2005 24th international conference on offshore mechanics and arctic engineering, 12–17, June, Halkidiki; 2005. doi:10.1115/OMAE2005-67294.

Nazir M, Khan F, Amyotte P. Fatigue reliability analysis of deep water rigid marine risers associated with Morison-type wave

loading. Stoch Environ Res Risk Assess. 2008;22(3):379–90. doi:10.1007/s00477-007-0125-2.

Pang DX, Liu QY, Meng QH, et al. Solving method for nonlinear contact problem of drill strings in 3D curved borehole. Acta Pet Sin. 2009;30(1):121–4 (in Chinese).

Park HI, Jung DH. A finite element method for dynamic analysis of long slender marine structures under combined parametric and forcing excitations. Ocean Eng. 2002;29(11):1313–25. doi:10.1016/S0029-8018(01)00084-1.

Song J, Lu L, Teng B, et al. Laboratory tests of vortex-induced vibrations of a long flexible riser pipe subjected to uniform flow. Ocean Eng. 2011;38(11):1308–22. doi:10.1016/j.oceaneng.2011.05.020.

Stomp RJ, Fraser GJ, Actis SC, et al. Deepwater DST planning and operations from a DP vessel. J Pet Technol. 2005;57(6):55–7. doi:10.2118/90557-MS.

Tognarelli M, Fontaine E, Beynet P, et al. Reliability-based factors of safety for VIV fatigue using field measurements. In: ASME 2010 29th international conference on ocean, offshore and arctic engineering, 6–11 June, Shanghai; 2010. doi:10.1115/OMAE2010-21001.

Triolo D, Mosness T, Habib R K. The Liwan gas project: a case study of South China Sea deepwater drilling campaign. In: The international petroleum technology conference, 26–28 March, Beijing; 2013. doi:10.2523/16722-MS.

Wang H, Sun J, Jukes P. FEA of a laminate internal buckle arrestor for deep water pipe-pipe flowlines. In: ASME 2009 28th international conference on ocean, offshore and arctic engineering, 31 May–5 June, Honolulu; 2009. doi:10.1115/OMAE2009-79520.

Wendler C, Scott M. Testing and perforating in the HPHT deep and ultra-deep water environment. In: The SPE Asia Pacific oil & gas conference and exhibition, 22–24 Oct, Perth; 2012. doi:10.2118/158851-MS.

Xie X, Fu JH, Zhang Z, et al. Mechanical analysis of deep water well testing strings. Nat Gas Ind. 2011;31(1):77–9 (in Chinese).

Xu LB, Jiang SQ, Zhou JL. Challenges and solutions for deep water drilling in the South China Sea. In: Offshore technology conference, 6–9 May, Houston; 2013. doi:10.4043/23964-MS.

Yang J, Liu CH, Liu HB, et al. Strength and stability analysis of deep sea drilling risers. Pet Sci. 2007;4(2):60–5. doi:10.1007/BF03187443.

Zeng ZJ, Hu WD, Liu JC, et al. A mechanical analysis of the gas testing string used in HTHP deep wells. Nat Gas Ind. 2010;30(2):85–7 (in Chinese).